Performance of Thomas–Fermi and linear response approaches in periodic two-dimensional systems

L Calderín and M J Stott

Department of Physics, Queen's University, Kingston, Ontario, K7 L 3N6, Canada

E-mail: calderin@physics.queensu.ca and stott@mjs.phy.queensu.ca

Abstract
A study of the performance of Thomas–Fermi and linear response theories in the case of a two-dimensional periodic model system is presented. The calculated density distribution and total energy per unit cell compare very well with exact results except when there is a small number of particles per cell, even though the potential has narrow tight-binding bands. The results supplement earlier findings of Koivisto and Stott for a localized impurity in a two-dimensional uniform gas.

PACS number: 71.15.Mb

(Some figures in this article are in colour only in the electronic version)

1. Introduction

The non-interacting electron gas has some interesting features for two dimensions which have consequences in density functional theory. Calculations have been reported for the electron distribution around a model impurity in a uniform, non-interacting two-dimensional electron gas for various Fermi energies [1–3], and for the total number of displaced particles and the total energy [3]. The results of these essentially exact calculations are in very good agreement with the results of linear response theory and the Thomas–Fermi (TF) approach even for impurity potentials strong enough to bind several electrons. This good agreement was first interpreted as a feature of linear response theory (LRT) [1, 2], but two dimensions played no special role in the argument. Later, it was argued that the success of the approximations depended not so much on the properties of linear response (LR) but on a special feature of all density response functions in two dimensions [3].

The TF approach gave similar and usually better agreement with the exact results than LRT and can be systematically corrected by adding terms that depend on the density gradients using the method of Kirzhnits [4–6]. This method obtains the non-interacting kinetic energy functional $T_s[n]$ of the electron density $n(\vec{r})$ as an expansion in density gradients with the

leading term being the TF result. The calculations are straightforward but very tedious. For three dimensions, corrections as far as the sixth order in gradients have been found [4, 5, 7], and results are not encouraging. Successive terms in the expansion $n[V]$ in gradients of the potential $V(\vec{r})$ contain increasing powers of $1/\sqrt{E_F - V(\vec{r})}$ and the series diverges badly for $E_F \sim V(\vec{r})$, near the classical turning point. However, the situation is very different in two dimensions for it was shown [3, 6, 8–10] that for $D = 2$ all density gradient corrections to the TF term calculated using the method of Kirzhnits [4–6] vanish at zero temperature.

The systems previously considered consisted of a single impurity in an otherwise uniform two-dimensional (2D) gas, and it is of interest to investigate the validity of the TF approach and LRT for a periodic 2D crystal, a model system more widely applicable. Further investigation of the kinetic energy density functional for a 2D system of electrons may also lead to successful approximations for 3D systems, which could be used in orbital-free-like methods for the simulations of large systems, which use an explicit density functional for the electron kinetic energy.

2. Model

2.1. Exact solution

The model we investigate is one first introduced and treated by Brillouin [12], Morse [13], MacColl [14] and Slater [15]. It consists of a two-dimensional electron gas in the presence of a separable periodic potential

$$V(\vec{r}) = 2W_1\left(1 - \cos\left(\frac{2\pi x_1}{c_1}\right)\right) + 2W_2\left(1 - \cos\left(\frac{2\pi x_2}{c_2}\right)\right), \tag{1}$$

where x_i are the 2D cartesian coordinates, W_i are the potential strength parameters and c_i are the unit cell parameters of a 2D rectangular unit cell; all in atomic units.

The Schrödinger equation for this problem separates, and reduces to one-dimensional Mathieu–Floquet equations [11] of the form

$$F''_{n,\nu_i}(z_i) + (a_n(\nu_i) - 2q_i\cos(2z_i))F_{n,\nu_i}(z_i) = 0, \qquad i = 1, 2; \tag{2}$$

where $F_{n,\nu_i}(z_i)$ is a solution for the band index n in terms of reduced coordinates z_i, potential strength q_i, wave vector ν_i and eigenvalues $a_n(\nu_i)$. The relationships between reduced variables and the coordinates x_i, potential strength W_i, unit cell parameters c_i and wave vector k_i of the system are $z_i = \pi x_i/c_i$, $\nu_i = \pi k_i/c_i$, $a_n(\nu_i) = 2c_i^2(\epsilon_n(k_i) - 2W_i)/\pi^2$ and $q_i = -2c_i^2 W_i/\pi^2$. The wavefunction and eigenvalue of the (lm)-state with wave vector $\vec{k}$ are respectively

$$\phi_{lm}(\vec{k}, \vec{r}) = F_{l,\nu_1(k_1)}(\pi x_1/c_1)F_{m,\nu_2(k_2)}(\pi x_2/c_2) \tag{3}$$

and

$$\epsilon_{lm}(\vec{k}) = \pi^2/2\big(a_l(\pi/c_1 k_1)/c_1^2 + a_m(\pi/c_2 k_2)/c_2^2\big) + 2(W_1 + W_2). \tag{4}$$

The ground-state electron density given by the sum over occupied states up to the Fermi energy, E_F, is

$$n(\vec{r}) = \frac{\Omega}{2\pi^2}\sum_{lm}\int_{BZ} d^2\vec{k}\,|\phi_{lm}(\vec{k}, \vec{r})|^2 \Theta(\epsilon_{lm}(\vec{k}) - E_F), \tag{5}$$

where Ω is the area of the unit cell, and $\Theta(x)$ is the step function. The total number of particles in the unit cell is $N = \int_{\Omega} d^2 r n(\vec{r})$, and the total energy per unit cell is

$$E = \frac{\Omega}{2\pi^2}\sum_{lm}\int_{BZ} d^2\vec{k}\,\epsilon_{lm}(\vec{k})\,\Theta(\epsilon_{lm}(\vec{k}) - E_F). \tag{6}$$

The object now is to compare the exact density distribution and total energy with the corresponding results calculated within linear response theory and the Thomas–Fermi approximation all for the same number of particles.

2.2. Linear response theory

In this approach [17] a uniform, non-interacting electron gas of density $\bar{n}$ is perturbed by the potential $V(\vec{r})$ and to first order, or in the so-called linear response theory, the density is given by

$$n_{\text{LR}}(\vec{r}) = \bar{n} + \frac{1}{\Omega} \sum_{\vec{q} \neq 0} \tilde{\chi}(\vec{q}) \tilde{V}(\vec{q}) \exp(-i\vec{q} \cdot \vec{r}) \tag{7}$$

where $\tilde{V}(\vec{q})$ is the Fourier transform of the potential, and $\tilde{\chi}(\vec{q})$ is the linear density response function, which in two dimensions is

$$\tilde{\chi}(\vec{q}) = \begin{cases} -\dfrac{1}{\pi} & \text{if} \quad q < 2k_F \\ -\dfrac{1}{\pi}\left(1 - \dfrac{\sqrt{x^2-1}}{x}\right) & \text{if} \quad q > 2k_F \end{cases} \tag{8}$$

where $k_F = \sqrt{2\pi\bar{n}}$ is the Fermi wave vector of the unperturbed gas and $x = q/2k_F$. The total ground state energy consistent with LRT is

$$E_{\text{LR}} = \frac{\pi}{2}\bar{n}^2\Omega + \frac{\bar{n}}{2} \int d^2r \, V(\vec{r}) + \frac{1}{2} \int d^2r \, n_{\text{LR}}(\vec{r}) \, V(\vec{r}). \tag{9}$$

If the $\vec{q}$-vectors of $V(\vec{q})$ all lie within a circle of radius $2k_F$, then the LR density reduces to

$$n_{\text{LR}}(\vec{r}) = \bar{n} - \frac{1}{\pi\Omega} \sum_{\vec{q} \neq 0} \tilde{V}(\vec{q}) \exp(-i\vec{q} \cdot \vec{r}) \tag{10}$$

$$= \frac{\pi\bar{n} + \bar{V} - V(\vec{r})}{\pi}, \tag{11}$$

where $\bar{V}$ is the average potential

$$\bar{V} \equiv \frac{1}{\Omega} \int_{\Omega} d^2r \, V(\vec{r}). \tag{12}$$

The corresponding LR total energy is given by

$$E_{\text{LR}} = \frac{\pi\Omega}{2}\bar{n}^2 + \Omega\bar{V}\bar{n} + \frac{\Omega}{2\pi}(\overline{V^2} - \overline{V}^2), \tag{13}$$

where $\overline{V^2} \equiv \int_{\Omega} d^2r \, V^2(\vec{r}) \, d^2r/\Omega$.

For the periodic potential given by (1) the density is

$$n_{\text{LR}}(\vec{r}) = \bar{n} - 2W_1 \tilde{\chi}\left(\frac{2\pi}{c_1}\right) \cos\left(\frac{2\pi}{c_1}x_1\right) - 2W_2 \tilde{\chi}\left(\frac{2\pi}{c_2}\right) \cos\left(\frac{2\pi}{c_2}x_2\right) \tag{14}$$

and the total number of particles per cell is $N = \Omega\bar{n}$. The total energy per cell is

$$E_{\text{LR}} = \frac{\pi\bar{n}^2\Omega}{2} + 2\bar{n}\Omega(W_1 + W_2) + \Omega\left(W_1^2 \tilde{\chi}\left(\frac{2\pi}{c_1}\right) + W_2^2 \tilde{\chi}\left(\frac{2\pi}{c_2}\right)\right). \tag{15}$$

If the wave vectors of the perturbing potential are such that π/c_1 and π/c_2 lie inside the Fermi circle, then

$$\bar{n} > \frac{\pi}{2} \max(1/c_1, 1/c_2)^2. \tag{16}$$

In this case the density and total energy become

$$n_{\mathrm{LR}}(\vec{r}) = \bar{n} + \frac{2W_1}{\pi} \cos\left(\frac{2\pi}{c_1} x_1\right) + \frac{2W_2}{\pi} \cos\left(\frac{2\pi}{c_2} x_2\right) \tag{17}$$

and

$$E_{\mathrm{LR}} = \frac{\pi \bar{n}^2 \Omega}{2} + 2\bar{n}\Omega(W_1 + W_2) - \Omega\frac{(W_1^2 + W_2^2)}{\pi}, \tag{18}$$

respectively.

2.3. Thomas–Fermi approximation

Within the Thomas–Fermi approximation for the kinetic energy the particle density is

$$n_{\mathrm{TF}}(\vec{r}) = \frac{E_F - V(\vec{r})}{\pi} \Theta[V(\vec{r}) - E_F], \tag{19}$$

and E_F is given in terms of the total number of particles per cell through $N = \int_{\Omega} \mathrm{d}^2 r \, n_{\mathrm{TF}}(\vec{r})$. The total energy per cell is

$$E_{\mathrm{TF}} = \frac{\pi}{2} \int_{\Omega} \mathrm{d}^2 \vec{r} \, [n_{\mathrm{TF}}(\vec{r})]^2 + \int_{\Omega} \mathrm{d}^2 \vec{r} \, n_{\mathrm{TF}}(\vec{r}) \, V(\vec{r}). \tag{20}$$

Now we consider the case of the Fermi energy above the potential so that $E_F > V_{\max}$; we have

$$n_{\mathrm{TF}}(\vec{r}) = \frac{E_F - V(\vec{r})}{\pi}, \tag{21}$$

which by integration over the cell gives for E_F in terms of the number of particles

$$E_F = \pi \bar{n} + \bar{V}. \tag{22}$$

Using (22) the condition $E_F > V_{\max}$ becomes

$$\bar{n} > \frac{(V_{\max} - \bar{V})}{\pi}. \tag{23}$$

Using (22) for E_F in (21) the expression for the TF density is the same as n_{LR} when $\bar{n} > q_{\max}^2/8\pi$ given by (11), and the total energy coincides with E_{LR} ((20)). We see that both LRT and TF give simple results for the density and the total energy when certain conditions are met: $\bar{n} > q_{\max}^2/8\pi$ for LRT and $E_F > V_{\max}$ for TF, and when both conditions are met the results are identical. This is not unexpected since LRT assumes a weak potential and when the potential is also slowly varying ($\pi \max(1/c_1, 1/c_2) < k_F$) the conditions are met for TF to work for a weak potential. However, for 2D the conditions are met abruptly because of the special form of $\tilde{\chi}(\vec{q})$.

For the potential given by (1) and $E_F > V_{\max}$ the TF Fermi energy is

$$E_F = \pi \bar{n} + 2(W_1 + W_2); \tag{24}$$

the LRT results for the density (17) and total energy (18) are obtained and the condition $E_F > V_{\max}$ becomes

$$\bar{n} > \frac{2(W_1 + W_2)}{\pi}. \tag{25}$$
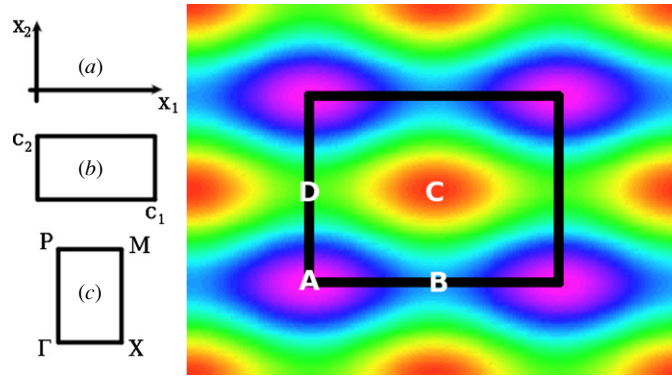
Figure 1. General view of the 2D periodic potential. (*a*) The system of reference (*b*) unit cell parameters and (*c*) irreducible Brillouin zone are shown on the left. The letters at the corners of the Brillouin zone label the following points: $\Gamma = (0, 0)$, $X = (\pi/c_1, 0)$, $M = (\pi/c_1, \pi/c_2)$ and $P = (0, \pi/c_2)$. A unit cell related to the potential is shown on the right as well as the following values of the potential: A: $V = 0$, B: $V = 4W_1$, C: $V = 4(W_1 + W_2)$ and D: $V = 4W_2$.

2.4. Calculations

Calculations of the exact, LR and TF densities and total energies as functions of the number of particles per cell have been performed for square and rectangular lattices. The real space integrals involved in both the exact and TF calculations used the trapezoidal rule with grids of 20×20 points in the unit cell. The exact calculations also required integrals over reciprocal space. These were performed sampling 20×20 points in the Brillouin zone with the Methfessel–Paxton S_{10} function [16] with a width of 0.01. Enough energy bands were considered to guarantee that all band overlaps were accounted for in the sums over bands in (5) and (6). For the largest number of electrons 81 bands were needed.

3. Results

An example of the periodic 2D potential is shown in figure 1 for a general rectangular lattice. The global minimum and zero of the potential is at the corners of the rectangular unit cell and its global maximum of $4(W_1 + W_2)$ is at the middle of the unit cell. There are saddle points with values of $4W_i$ at the centers of the sides of the unit cell which provide the barriers for an electron moving from one cell to the next.

The exact band structure is shown in figure 2 for a rectangular lattice with unit cell parameters $c_1 = 4.443$ and $c_2 = 3.141$, and potential strengths $W_1 = 1$ and $W_2 = 2$. The corresponding density of states (DOS) with a Gaussian broadening to help visibility is also shown. The very narrow band at $\sim$2.7 Ha involves tunneling through a classically forbidden region between cells in all directions. The band at $\sim$4.5 Ha, slightly above the 4 Ha saddle point at B, also shows very little dispersion. The next higher bands show dispersion along the ΓX directions due to propagation in the x_1 direction over the lower saddle point at B. There is a small band gap at $\sim$6 Ha but there are band overlaps at all energies above this.

Narrow localized states are seen below the potential barriers along the sides, while above the bands show a free electron-like character, which is more accentuated for higher Fermi energies. There is more dispersion along the Γ–X and M–P lines than along X–M and P–Γ lines because the former are in the x_1 direction in real space, while the latter are along x_2.
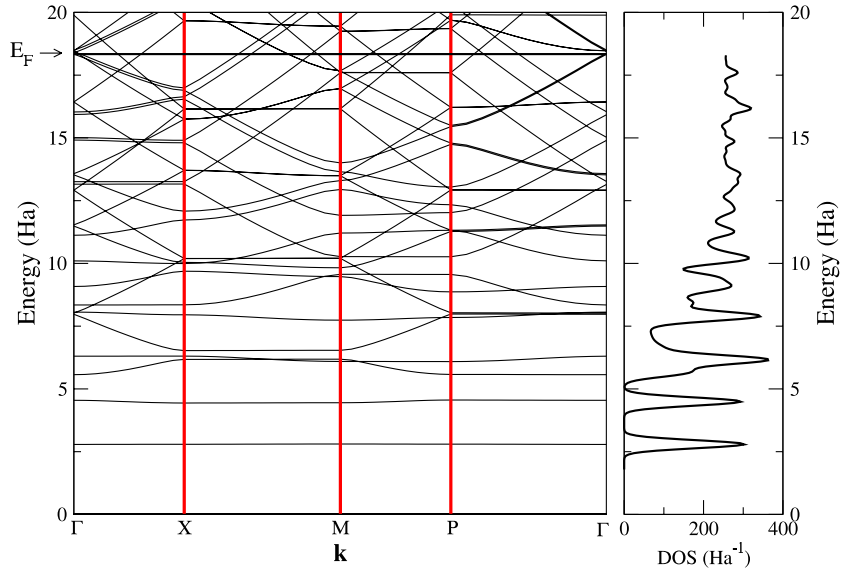
Figure 2. Band structure and DOS for a rectangular lattice $c_1 = 4.443$ and $c_2 = 3.141$, and potential strengths $W_1 = 1$ and $W_2 = 2$.

Therefore, the greater dispersion along the Γ–X and X–P lines is a consequence of the lower potential barrier along that direction (figure 1, label B) than along x_2 (figure 1, label D). The DOS also shows two narrow, tightly bound states—most of the widths are artificial due to the sampling—and an increasingly free particle character above as evidenced by the flat DOS.

    Illustrations of density distributions are shown in figures 3 and 4. The exact, LRT and TF densities are shown for two cases. The first, figure 3 is for a small number of particles (≈ 2) in tightly bound states. The exact and TF results have islands concentrated in the corners of the unit cell where the potential is a minimum. Whereas the exact density has a smooth distribution between the islands, the TF density falls abruptly to zero for values of the potential below its Fermi energy. In contrast, LRT fails to account for the tightly bound states. It becomes negative at the center of the cell around the potential maximum, and the islands are misshapen. The case with a larger number of particles (≈ 30) is shown in figure 4. The TF Fermi energy is above the potential maximum and the TF and LRT densities are identical and quantitatively and qualitatively very similar to the exact density.

    In order to compare the densities in more detail we show in figure 5 the standard deviation of the approximate densities (n_a), with respect to the exact one (n_e) over the rectangular unit cell as functions of the average density:

$$\sigma = \sqrt{\int_\Omega d^2 r (n_e - n_a)^2 / \Omega}. \tag{26}$$

The results show TF performing better than LRT for small numbers of particles as noted earlier, but the discrepancies for both are small as E_F for the exact model approaches the potential maximum and diminish rapidly as E_F increases further. TF and LRT give identical densities for $\bar{n} > 2(W_1 + W_2)/\pi$.

    The total energy calculated as a function of the number of particles for a square lattice with a unit cell parameter of 4.443 and potential strength of 1 is shown in figure 6(a), and for a

(a) Exact density   (b) LR density   (c) TF density
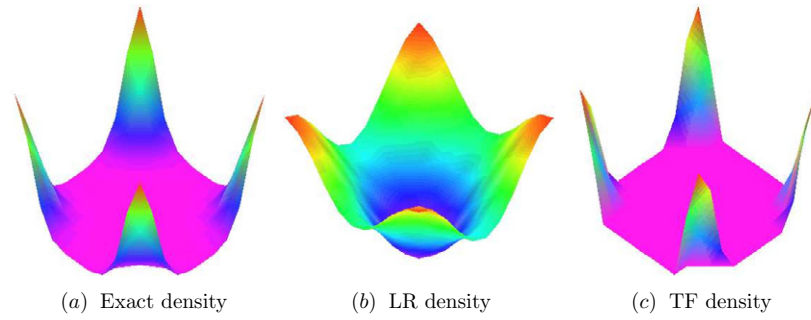
Figure 3. Typical densities for a small average density, $\bar{n} = 0.07$, which for the exact model corresponds to a Fermi energy $E_F = 2.8$ which is below the maximum of the potential.

(a) Exact density   (b) LR density   (c) TF density
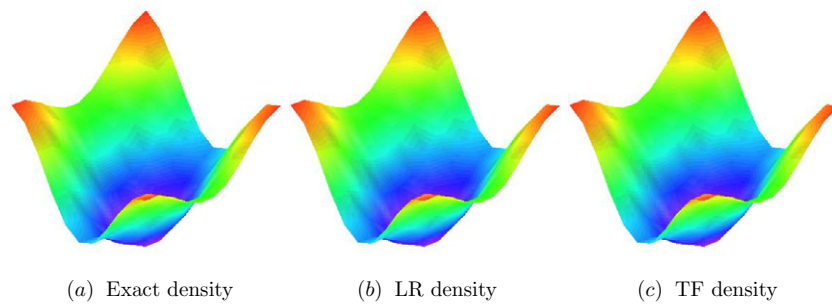
Figure 4. Typical densities for a large average density, $\bar{n} = 2.1$, which for the exact model corresponds to a Fermi energy $E_F = 12.5$ which is above the maximum of the potential.
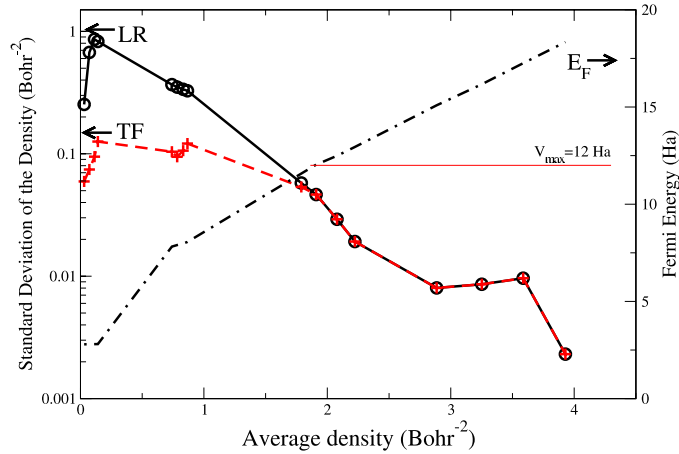
Figure 5. Standard deviation, σ, of the approximate densities respect to the exact one for different mean particle density for the the rectangular lattice ($c_1 = 4.443$, $c_2 = 3.141$, $W_1 = 1$, $W_2 = 2$). The Fermi energy of the exact system is also shown with a line marking the maximum of the potential at 12 Ha.

rectangular lattice with unit cell parameters $c_1 = 4.443$ and $c_2 = 3.142$ and potential strengths $W_1 = 1$ and $W_2 = 2$ in figure 6(b). The exact results as well as the LRT and TF results are

7

(a) $c_1 = 4.443$ and $W_1 = 1$.

(b) $c_1 = 4.443$, $c_2 = 3.141$, $W_1 = 1$ and $W_2 = 2$.
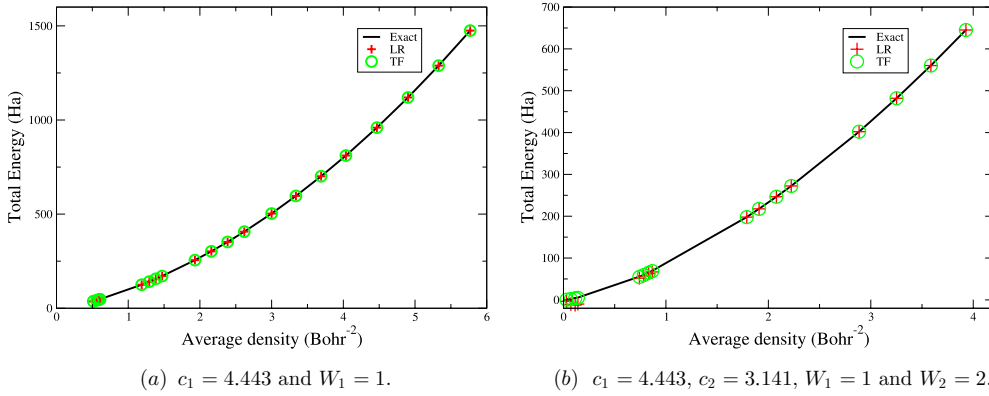
Figure 6. Total energy versus average density for (*a*) a square (*b*) and rectangular two-dimensional lattices.

shown. There is very good agreement between the exact and the approximate results even for Fermi energies of the exact model below the global maximum of the potential at 12 Ha. The slightly poorer agreement for the rectangular lattice is due to less band overlap.

4. Discussion and conclusions

Previous numerical studies [3] of the ground state of a localized impurity in a 2D noninteracting uniform gas showed that the impurity energy, displaced density distribution and the number of displaced particles calculated within TF and LRT were in very good agreement with exact results. This prompted the present work which investigated if there might be the same agreement for an extended 2D system. A 2D model with a periodic sinusoidal potential has been studied and the particle density distribution and total energy as functions of the mean density calculated within the LRT and TF approximations are found to be in very good agreement with the exact quantities except for LRT when there is a small number of particles per unit cell. For example, the LRT density is negative in some of the cell. Moreover, the two sets of approximate quantities are identical for some mean density which depends on the strength of the potential and its Fourier wave vectors, and converges very rapidly onto the exact results as the mean density increases further.

Corrections to LRT involve the quadratic and higher order response functions that for 2D systems have been studied by Zhang [18]. When the potential has no short wavelength Fourier components and $E_F > V_{max}$, TF and LRT results coincide and TF can be corrected to include density inhomogenieties by adding gradient corrections using, for instance, the Kirzhnits approach [4–6]. But, for 2D all density gradient corrections calculated in this fashion vanish at zero temperature [3, 6, 8–10]. This is not to claim that TF is exact for 2D because we know that it misses Fermi surface effects such as Friedel oscillations and the effects of short wavelength variations in the potential, but the vanishing of the gradient corrections may account for the success of TF for 2D, and of LRT when they coincide.

Both potentials studied in some detail: the Gaussian impurity potential earlier [3] and the sinusoidal periodic potential, here, are smooth (the Fourier components of the Gaussian potential decay very rapidly and the sinusoidal potential has no Fourier components for $q > \pi \max(1/c_1, 1/c_2)$). It comes to mind that TF may work well if the potential is free of

singularities such as a Coulomb singularity or a discontinuity, and 2D systems may not be as special as they appear from the present results. A supporting point may be that the Kirzhnits method [4–6] begins by finding expansions of the density and the kinetic energy in gradients of the potential and then eliminates these to obtain an expansion of the kinetic energy in gradients of the density. The intermediate step involving gradients of the potential is problematic if not all gradients exist, again, such as for a Coulomb singularity or a discontinuous potential, but there may be methods that avoid this intermediate step.

Further investigation of the validity of the TF approximation for 2D is warranted. The demonstrated accuracy of TF for a localized impurity [1–3] and now for an extended periodic system is approaching useful levels. The formulation of corrections to TF accounting for short wavelength components of the potential and Fermi surface effects would allow a very simple orbital-free *ab initio* simulation method for 2D systems, but might also shed light on properties of an explicit density functional of the electron kinetic energy for 3D systems.

Acknowledgment

References

[1] Zaremba E, Nagy I and Echenique P M 2003 *Phys. Rev. Lett.* **90** 046801
[2] Zaremba E, Nagy I and Echenique P M 2005 *Phys. Rev.* B **71** 125323
[3] Koivisto M and Stott M J 2007 *Phys. Rev.* B **76** 195103
　　Koivisto M and Stott M J 2008 *Phys. Rev.* B **77** 199902 (erratum)
[4] Kirzhnits D A 1957 *Sov. Phys.—JETP* **5** 64
[5] Hodges C H 1973 *Can. J. Phys.* **51** 1428
[6] Brack M and Bhaduri R K 2003 *Semiclassical Physics* (Reading, MA: Addison-Wesley)
[7] Murphy D R 1981 *Phys. Rev.* A **24** 1682
[8] Shao Jiushu 1993 *Mod. Phys. Lett.* B **7** 1193
[9] Geldart D J W and Gumbs G 1986 *Phys. Rev.* B **33** 2820
[10] Salasnich L 2007 *J. Phys. A: Math. Theor.* **40** 9987
[11] Abramowitz M and Stegun I A (eds) 1972 *Handbook of Mathematical Functions with Formulas, Graphs, and Mathematical Tables* (New York: Dover)
[12] Brillouin L 1930 *J. Phys. Radium* **1** 377
[13] Morse P M 1930 *Phys. Rev.* **35** 1310
[14] MacColl L A 1951 *Bell Syst. Tech. J.* **30** 888
[15] Slater J C 1952 *Phys. Rev.* **87** 807
[16] Methfessel M and Paxton A T 1989 *Phys. Rev.* B **40** 3616
[17] Ziman J M 1964 *Principles of the Theory of Solids* (Cambridge: Cambridge University Press)
[18] Zhang M Q 1991 *J. Math. Phys.* **32** 1344